

文章编号 1004-924X(2009)10-2392-09

由相关函数拟合极值法提高位相板 衍射光斑定位的计算效率

郎治国, 谭久彬

(哈尔滨工业大学 超精密光电仪器工程研究所, 黑龙江 哈尔滨 150001)

摘要: 为了提高相关函数拟合极值法在二维位相板衍射光斑亚像素定位中的计算效率, 对相关函数拟合极值法中的模板大小、拟合窗口大小及相关函数 3 种影响因素进行了分析。分析过程以仿真图像检验法为理论基础, 即用数学仿真图像验证算法和程序的可靠性和精度。分析结果表明, 3 种影响因素均对计算效率产生较大影响, 整像素搜索时模板和拟合窗口大小的选取对定位精度影响最大。同理, 对二维位相板衍射光斑亚像素定位实验中的搜索模板和拟合窗口大小进行了优化设计, 最佳模板大小为 51 pixel \times 51 pixel, 最佳拟合窗口大小为 3 pixel \times 3 pixel, 与选用恰好包含整个衍射光斑时的模板(131 pixel \times 131 pixel)相比, 整个定位过程的计算时间缩短了 40%, 在不损失定位精度的同时有效提高了计算效率。

关键词: 衍射光斑; 计算效率; 亚像素定位; 相关函数; 拟合窗口

中图分类号: O436.1 **文献标识码:** A

Improvement of calculation efficiency for locating diffraction spot of phase plate with correlation function fitting extreme method

LANG Zhi-guo, TAN Jiu-bin

(*Institute of Ultra-precise Optoelectronic Instrument Engineering,
Harbin Institute of Technology, Harbin 150001, China*)

Abstract: In order to improve the computational efficiency of sub-pixel location of a diffraction spot generated by a two-dimensional phase plate with the correlation function fitting extreme method, three effect factors, the template size, fitting window size and the correlation function were analyzed in detail. On the basis of the theory of emulation image examination, mathematical emulation images were used to verify the reliability and accuracy of algorithms and programs. Analyzing results indicate that the three effect factors all have bigger effect on computational efficiency and the template and fitting window sizes show the biggest effect on the locating precision during integer pixel searching. The optimal design of searching template and fitting window sizes are completed during the sub-pixel location experiment of diffraction spot generated by the two-dimensional phase plate, It is shown that the optimized template and fitting window sizes are 51 pixel \times 51 pixel and 3 pixel \times 3 pixel, respectively. Comparing with the template of 131 pixel \times 131 pixel which just includes the whole diffraction spot,

收稿日期: 2008-10-29; 修订日期: 2008-12-02.

基金项目: Supported by the National Natural Science Foundation of China (Grant No. 60878028)

the calculating time of whole locating process is shortened by 40%, which shows the computational efficiency is improved without degrading location precision.

Key words: diffraction spot; computational efficiency; sub-pixel location; correlation function; fitting window

1 Introduction

A digital Image Correlation (DIC) method is presented respectively by a Japanese named I. Yamaguchi and Americans named W. H. Peters, W. F. Panson *et al.* who worked in University of South Carolina^[1-3]. The correlation function of two maps of the laser speckle before and after distorting of an object is calculated, and then the displacement and deforming of the measured object can be obtained. Comparing with laser interference measurement, it has the advantages of the simple measurement system and low requirement for environment *etc.*. After developing and improving of more than twenty years, the DIC method has been a common optical measurement mean and applied in experimental mechanics and other science research and engineering fields. As one of DIC measurement methods, the correlation function fitting extreme method has been widely adopted in factual applications because of its advantages in high noise-immunity, high precision and so on, such as measuring vibration and deformation of electric devices, and the deformation of rocks^[4-9]. Theory of correlation function fitting method is simple, its important problem in practical applications is how to improve calculating precision and efficiency. In addition, previous emphasis of research work was put on selecting of correlation functions, for example, Ma. S. P *etc.* has discussed ten kinds of correlation functions in detail^[10]. But other effect factors influencing location precision and computational efficiency in this method has not been analyzed. In factual application, different correlation coefficient matrixes are obtained because different correlation

functions and searching templates are adopted when an integer pixel displacement is calculated by the correlation searching method. So for the same calculated sub-pixel displacement, the calculation results and efficiencies by correlation function fitting extreme method must be different. In addition, different fitting windows also have effects on calculation results and efficiencies when the correlation coefficient matrixes are fitted with the curve surface.

In order to improve the computational efficiency of sub-pixel location of a diffraction spot generated by a two-dimensional phase plate by the correlation function fitting extreme method, the above effect factors are analyzed in detail and the analyzing process is based on an emulation image examination method. Analyzing results show that the three effect factors all have bigger effects on the computational efficiency and the template and fitting window sizes show the biggest effect on locating precision during the integral pixel searching. The optimum design of searching template and fitting window sizes is completed during the sub-pixel location experiment of a diffraction spot generated by the two-dimensional phase plate. Experimental results show that the calculating time of whole location process is shorted by 40% through selecting optimal template and fitting window sizes, and the computational efficiency is improved without degrading location precision.

2 Correlation function fitting extreme method

2.1 Basic principle of digital image correlation

In DIC method, the target position (for im-

age sequence, the first picture or previous picture of current image is adopted) of an image with known target characters is defined first of all, then a gray matrix of $(2M+1) \times (2M+1)$ pixel with center (m, n) is regarded as a searching template. At last, a correlation function is adopted to calculate correlation results in the im-

age region including target points to be decided, and then the correlation function matrix can be obtained. At present, the common correlation functions with better results are as follows^[11]:

(1) Standard correlation function with sampling interval $[0, 1]$

$$C_2(m, n) = \frac{\sum_{i=-M}^M \sum_{j=-M}^M f(i, j) \cdot g(i+m, j+n)}{\sqrt{\sum_{i=-M}^M \sum_{j=-M}^M f^2(i, j) \cdot \sum_{i=-M}^M \sum_{j=-M}^M g^2(i+m, j+n)}}, \quad (1)$$

(2) Covariance (mean normalizing) correlation function

$$C_1(m, n) = \sum_{i=-M}^M \sum_{j=-M}^M [f(i, j) - f_{\text{mean}}][g(i+m, j+n) - g_{\text{mean}}], \quad (2)$$

(3) Standard covariance correlation function with sampling interval $[-1, 1]$

$$C_3(m, n) = \frac{\sum_{i=-M}^M \sum_{j=-M}^M [f(i, j) - f_{\text{mean}}][g(i+m, j+n) - g_{\text{mean}}]}{\sqrt{\sum_{i=-M}^M \sum_{j=-M}^M [f(i, j) - f_{\text{mean}}]^2 \sum_{i=-M}^M \sum_{j=-M}^M [g(i+m, j+n) - g_{\text{mean}}]^2}}, \quad (3)$$

Where $C(m, n)$ is the correlation function, $f(i, j)$ is the source image target lying in, $g(i, j)$ is the searching template (length of template is usually odd), f_{mean} and g_{mean} are the mean values of $f(i, j)$ and $g(i, j)$ respectively in corresponding autocorrelation windows. The template only moves in integral pixel when correlation functions described in formula (1) to (3) are adopted to search because only discrete gray information is recorded by digital image. So integral pixel correlation searching only locates a target image in integral pixel, and sub-pixel location method must be adopted for further improving location precision.

2.2 Solution principle of sub-pixel displacement by correlation function fitting extreme method

Because correlation function matrix is similar to the Gauss distribution in single-peaked region with maximum (m', n') as center, so the analytic curved surface function in this region can be obtained by the fitting method and the ex-

treme point of curved surface is regarded as the sub-pixel position of target point.

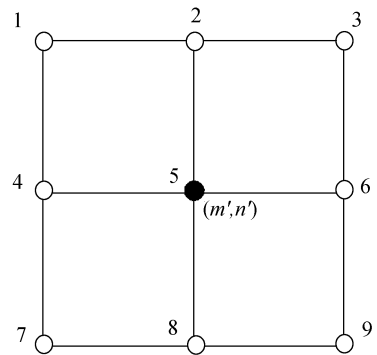


Fig. 1 Peak point and its eight adjacent points

As shown in Fig. 1, peak values around (m', n') searched by the integral pixel displacement may be expressed by the following binary quadric function:

$$C(m_i, n_i) = a_0 + a_1 m_i + a_2 n_i + a_3 m_i^2 + a_4 m_i n_i + a_5 n_i^2, \quad (4)$$

For fitting window of $k \times k$ (k usually equals

3, 5 or 7), a non-homogeneous linear equation set with undetermined coefficients a_0, \dots, a_5 is obtained by introducing coordinates of every point in

formula (4), so the least square method may be used to solve it. For example, for fitting window of 3×3 , the equation set may be written as:

$$\begin{bmatrix} \sum_{i=1}^9 1 & \sum_{i=1}^9 m_i & \sum_{i=1}^9 n_i & \sum_{i=1}^9 m_i^2 & \sum_{i=1}^9 m_i n_i & \sum_{i=1}^9 n_i^2 \\ \sum_{i=1}^9 m_i & \sum_{i=1}^9 m_i^2 & \sum_{i=1}^9 m_i n_i & \sum_{i=1}^9 m_i^3 & \sum_{i=1}^9 m_i^2 n_i & \sum_{i=1}^9 m_i n_i^2 \\ \sum_{i=1}^9 n_i & \sum_{i=1}^9 m_i n_i & \sum_{i=1}^9 n_i^2 & \sum_{i=1}^9 m_i^2 n_i & \sum_{i=1}^9 m_i n_i^2 & \sum_{i=1}^9 n_i^3 \\ \sum_{i=1}^9 m_i^2 & \sum_{i=1}^9 m_i^3 & \sum_{i=1}^9 m_i^2 n_i & \sum_{i=1}^9 m_i^4 & \sum_{i=1}^9 m_i^3 n_i & \sum_{i=1}^9 m_i^2 n_i^2 \\ \sum_{i=1}^9 m_i n_i & \sum_{i=1}^9 m_i^2 n_i & \sum_{i=1}^9 m_i n_i^2 & \sum_{i=1}^9 m_i^3 n_i & \sum_{i=1}^9 m_i^2 n_i^2 & \sum_{i=1}^9 m_i n_i^3 \\ \sum_{i=1}^9 n_i^2 & \sum_{i=1}^9 m_i n_i^2 & \sum_{i=1}^9 n_i^3 & \sum_{i=1}^9 m_i^2 n_i^2 & \sum_{i=1}^9 m_i n_i^3 & \sum_{i=1}^9 n_i^4 \end{bmatrix} \begin{bmatrix} a_0 \\ a_1 \\ a_2 \\ a_3 \\ a_4 \\ a_5 \end{bmatrix} = \begin{bmatrix} \sum_{i=0}^9 C_i \\ \sum_{i=0}^9 C_i m_i \\ \sum_{i=0}^9 C_i n_i \\ \sum_{i=0}^9 C_i m_i^2 \\ \sum_{i=0}^9 C_i m_i n_i \\ \sum_{i=0}^9 C_i n_i^2 \end{bmatrix}, \quad (5)$$

The extreme point of fitted curve surface of function $C(m, n)$ meets the following equation set:

$$\begin{cases} \frac{\partial C(m, n)}{\partial m} = a_1 + 2a_3 m + a_4 n = 0 \\ \frac{\partial C(m, n)}{\partial n} = a_2 + 2a_5 n + a_4 m = 0 \end{cases}, \quad (6)$$

Through solving the above equation set, the coordinate of extreme point of fitting curve surface is as follows

$$\begin{cases} m' = \frac{2a_1 a_5 - a_2 a_4}{a_4^2 - 4a_3 a_5} \\ n' = \frac{2a_2 a_3 - a_1 a_4}{a_4^2 - 4a_3 a_5} \end{cases}, \quad (7)$$

3 Effect factors of sub-pixel location precision and computational efficiency by two-dimensional phase plate diffraction spot

According to the basic principle of correlation function fitting extreme method, the main effect factors of sub-pixel location precision and computational efficiency of two-dimensional

phase plate diffraction spot is as follows: (1) the size of searching template. (2) the size of fitting window. (3) selection of correlation functions. Considering the basic principle of emulation image examination, the diffraction spot generated by two-dimensional phase plate is discussed above all.

3.1 Diffraction diagram by two-dimensional phase plate

In order to improve the gray gradient and contrast of the measurement spot, the two-dimensional phase plate is applied in a typical $f\theta$ measurement system. Furthermore, the sub-pixel location precision and image noise-immune of target image are improved, the specific analyses can be seen in literature^[12]. The phase structure of two-dimensional phase plate is as follows

$$T(x, y) = \begin{cases} 1, & \begin{cases} 0 < x < +\infty, 0 < y < +\infty \\ -\infty < x < 0, -\infty < y < 0 \end{cases} \\ e^{-in}, & \begin{cases} -\infty < x < 0, 0 < y < +\infty \\ 0 < x < +\infty, -\infty < y < 0 \end{cases} \end{cases}, \quad (8)$$

A diffraction spot diagram generated by a computer is shown in Fig. 2, where the wave-

length of incident beam is 632.8 nm and the focal length of Fourier lens is 400 mm. It can be seen that optical intensity distribution of the diffraction is centrosymmetric, furthermore contrast and gray gradient are improved largely comparing with those of Gauss measurement spots^[12].

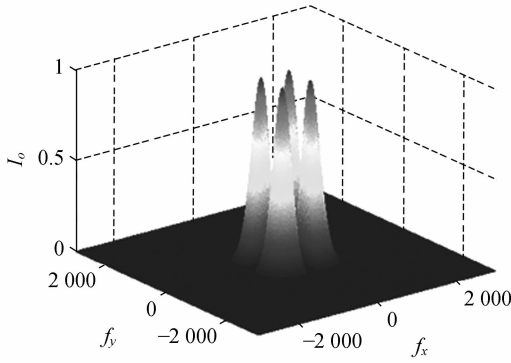


Fig. 2 Numerical emulation diagram of diffraction spot by two-dimensional phase plate

3.2 Effect of template size

The template size is a key parameter of DIC method. When integral pixel displacement is searched by the same correlation function, on the one hand, the template size is smaller, the calculation amount is smaller and computational efficiency is higher. But correlation coefficients of adjacent points around peak value point (m' , n') will vary acutely and capacity of noise-immune degrades. On the other hand, the bigger template may decrease effect of noise and make calculated correlation coefficients of adjacent points vary gently, but calculation amount increases. When a target image is moved for 0.5 pixel in m direction, the distribution diagram of calculated correlation coefficients in m direction by standard correlation function with different template sizes is shown in Fig. 3. Here the Gauss white noise of $N(0, 1)$ distribution with Signal-to-noise Ratio (SNR) 45 dB is added to the image^[13]. The spin filtering method is applied to noised-image^[14] (the same level noise and

image filtering method are adopted in following process of analyzing, and the adopted correlation functions are all standard correlation function). It can be seen from Fig. 3, the distribution of correlation coefficients differs a lot when different templates are used. When template size varies from 11 pixel \times 11 pixel to 41 pixel \times 41 pixel, the correlation coefficients vary acutely, but the correlation coefficients vary gently when the template size is larger than 41 pixel \times 41 pixel. So the coordinate of extreme point by correlation function fitting extreme method based on above correlation coefficient matrixes must differ a lot.

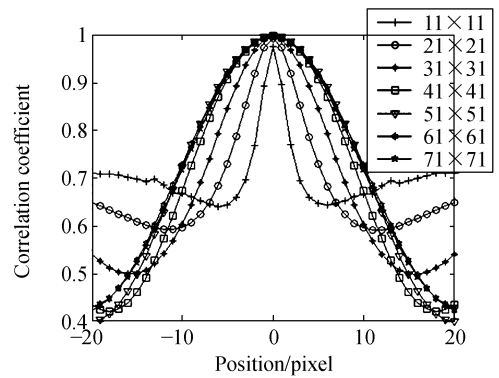


Fig. 3 Correlative coefficients by different templates during integral pixel searching

For further indicating effect of template size on location precision, Fig. 4 shows the sub-pixel location errors of different template sizes with fitting window size of 3 pixel \times 3 pixel when dif -

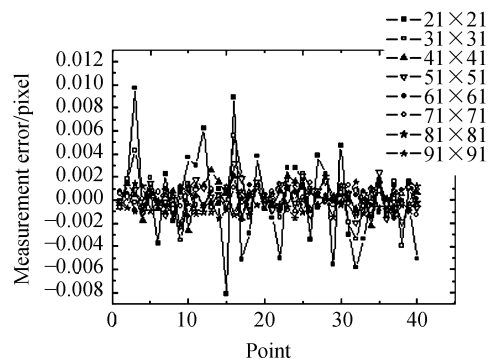


Fig. 4 Calculated displacements by different templates during integral pixel searching

fraction spot is moved in m direction. It is easy to see that the fluctuation range of location errors becomes smaller and smaller and convergent with the template size increasing.

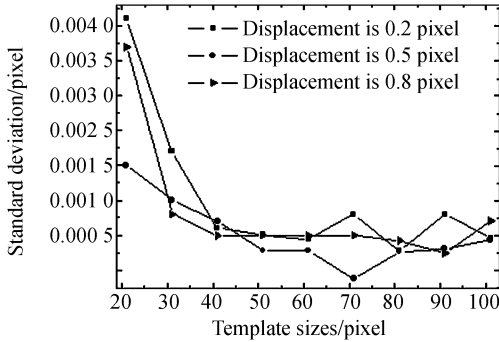


Fig. 5 Effect of different template sizes on calculated results of sub-pixel displacement

The calculated uncertainty (calculate for ten times for every template) of displacement by different template sizes is shown in Fig. 5 when diffraction spot is moved for 0.2, 0.5 and 0.8 pixel in m direction. It can be seen that sub-pixel location uncertainty becomes smaller and smaller, calculated and true displacements are convergent when template size becomes bigger and bigger from 21 pixel \times 21 pixel to 101 pixel \times 101 pixel. The calculation results convergences obviously and drives to stabilization when template size is bigger than 41 pixel \times 41 pixel. The relation between single location time and template size is shown in table. 1 when spot is moved for 0.5 pixel in m direction, where the fitting window size is 3 pixel \times 3 pixel. It is concluded that increasing template size only increase the calculation amount without improving sub-pixel location precision obviously. According to above analyses, for diffraction spot shown in Fig. 2, the optimal size of searching template is 41 pixel \times 41 pixel and the calculation time can be shortened effectively without losing location precision.

Tab. 1 Effect of template sizes on sub-pixel displacement calculation results (unit: pixel)

Template size/pixel	Calculation time/s
21 \times 21	22.8
31 \times 31	23.8
41 \times 41	24.9
51 \times 51	25.9
61 \times 61	31.7
71 \times 71	32.4
81 \times 81	34.7
91 \times 91	38.6
101 \times 101	42.5

3.3 Effect of fitting window size

In correlation function fitting extreme method, the sizes of fitting window are commonly 3 pixel \times 3 pixel, 5 pixel \times 5 pixel or 7 pixel \times 7 pixel. The sub-pixel location error curves are shown in Fig. 6 when a set of given displacements distributed homogeneously in interval $[0.1, 1.0]$ (pixel) with separation of 0.1 pixel, where the template size is 41 pixel \times 41 pixel and fitting windows are 3 pixel \times 3 pixel, 5 pixel \times 5 pixel and 7 pixel \times 7 pixel respectively. It can be seen that the location precision is the best when size of fitting window is 3 pixel \times 3 pixel. For single time sub-pixel location, the mean calculation time is 24.7 s, 25.5 s and 26.2 s respectively when the above three fitting windows are adopted. It is concluded that the

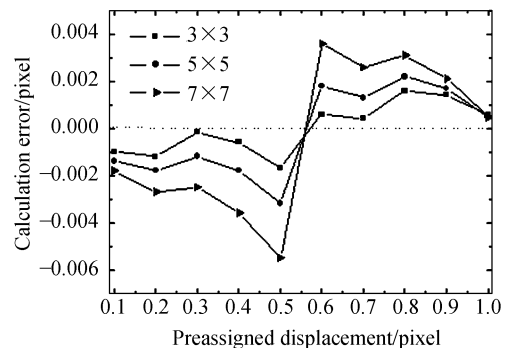


Fig. 6 Calculated errors of sub-pixel displacement when different fitting windows are adopted

optifitting window size should be $3 \text{ pixel} \times 3 \text{ pixel}$, and increasing the template size not only increase the calculation amount but also degrade the calculation precision.

3.4 Effect of correlation functions

In process of searching an integral pixel displacement, the correlation coefficient matrix of points around target points (m' , n') is different when correlation functions are different. For set of given standard displacements, which are distributed uniformly in interval $[0.1, 1.0]$ (pixel) and the distance between two adjacent points is 0.1 pixel, the sub-pixel location error by the three correlation functions described in section 2.1 is shown in Fig. 7. Every given standard displacement is all calculated for ten times, where the template size is $41 \text{ pixel} \times 41 \text{ pixel}$ and the fitting window size is $3 \text{ pixel} \times 3 \text{ pixel}$. According to data shown in Fig. 7, the biggest location error by different correlation functions is 3.94×10^{-4} pixel, so it is concluded that the effect of selection of commonly used correlation functions described in this paper is minute and even be neglected. But considering calculation amount, for single location, the calculation time by above three correlation functions is 25.67, 28.1 and 35.9 s respectively. The calculation amount of correlation function C_1 is less than that of C_2 and calculation amount of correlation function C_2 is less than that of C_3 . Consequently the correla-

tion function C_1 is selected to improve computational efficiency without degrading measurement precision.

4 Experimental verification

The experimental equipment is shown in Fig. 8, where the two-dimensional phase plate is applied in the typical $f-\theta$ measuring system and the measurement spot received by the target plane of CCD is a diffraction spot. Then the measurement results by the this equipment are compared with those by the SZY-99 photoelectric auto-collimator. The experimental conditions are as follows: the temperature of environment is $20.0 \text{ }^\circ\text{C}$ and relative humidity is 60%; the measurement range of SZY-99 photoelectric auto-collimator is $\pm 20''$, the measurement resolution and measurement precision are $0.01''$ and $\pm 0.1''$ respectively; the focal length of FT lens is 400 mm; the image detector is MV-1300UM monochrome industrial digital camera with a pixel size of $5.2 \text{ } \mu\text{m} \times 5.2 \text{ } \mu\text{m}$, the resolution is $1280 \text{ pixel} \times 1024 \text{ pixel}$ and SNR is bigger than 45 dB; light resource is linearly polarized He-Ne laser with a wavelength of 632.8 nm and the diameter of measurement basis beam is 1 mm; the CPU of computer is AMD 4400+ and the memory is 1G(DDR 667).

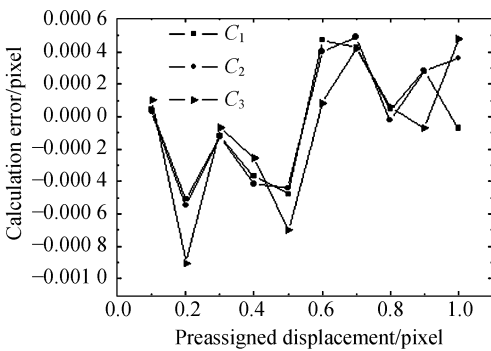


Fig. 7 Calculated errors of sub-pixel displacement when different correlation functions are adopted

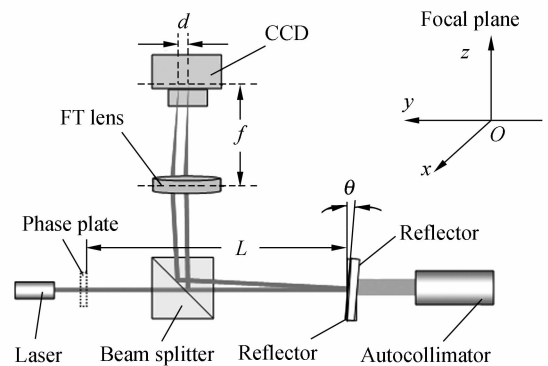


Fig. 8 Schematic diagram of typical $f-\theta$ system

The factual measured diffraction pattern by two-dimensional phase plate is shown in Fig. 9.

It is seen that the four diffraction peak values are not identical because the center of two-dimensional is not coincident with that of collimated beam completely which is called a centering error. The factual measured diffraction spot with size of $131 \text{ pixel} \times 131 \text{ pixel}$ is bigger than emulation spot shown in Fig. 2 because of the divergence angle of beam *etc.*. There exists minute difference in the high frequency-domain between factual diffraction spot and theoretical intensity distribution shown in Fig. 2, it is because that the aperture effect of optical elements in the system is neglected in the process of emulation.

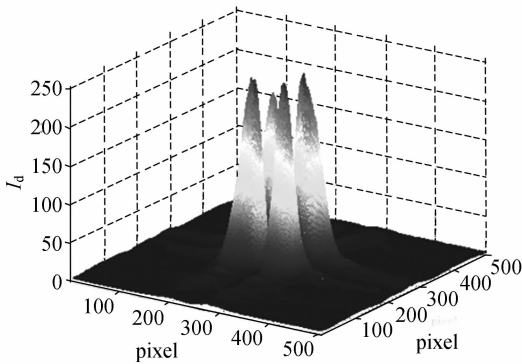


Fig. 9 Factual diffraction spot

According to above analyzing method, for factual measured diffraction spot shown in Fig. 9, the optimal template size is $51 \text{ pixel} \times 51 \text{ pixel}$, the optimal fitting window size is $3 \text{ pixel} \times 3 \text{ pixel}$ and the selected correlation function is standard correlation function C_1 . The experimental comparison results show that the angle measurement uncertainty of factual $f-\theta$ measurement system is $0.33''$ and the converted sub-pixel location uncertainty of diffraction spot is 0.09 pixel based on the theoretical formula of $f-\theta$

measurement system, and the single location time is 144 s. Furthermore the sub-pixel location uncertainty is still 0.09 pixel when the whole diffraction spot is included in the template of $131 \text{ pixel} \times 131 \text{ pixel}$, and the single location time is 241 s. It is concluded that the calculation time can be shorted by 40% without losing sub-pixel location precision.

5 Conclusions

In this paper, the three effect factors influencing on the location precision of a two-dimensional phase plate diffraction spot based on the correlation function fitting extreme method are discussed in detail. The analyzing results show that the effect of template and fitting window sizes on location precision is the biggest, but the effect of selection of commonly used correlation functions on location precision is minute, and the three effect factors all put bigger effects on computational efficiency. According to above conclusions, the diffraction spot generated by two-dimension phase plate in a comparison experiment is designed optimally. The optimal template size is $51 \text{ pixel} \times 51 \text{ pixel}$, the optimal fitting window size is $3 \text{ pixel} \times 3 \text{ pixel}$ and the selected correlation function is a standard correlation function shown in formula(2). According to above optimal designing results, the single location time is shorted by 40% without the degrading location precision of diffraction spot generated by two-dimension phase plate, so it is important to improve factual measurement efficiency.

References:

- [1] DENG L H, ZHU H M, WU Y Y. A study on the in-plane rotation measurement of a rigid object with the ultrasonic speckle correlation method [J]. *Journal of Experimental Mechanics*, 2006,21(6): 721-726. (in Chinese)
- [2] YAMAGUCHI I. Speckle displacement and de-

- formation in the diffraction and image fields for small object deformation [J]. *Opt. Acta*, 1981,28 (10):1359-1376.
- [3] PETERS W H, RANSON W F. Digital imaging techniques in experimental mechanics [J]. *Opt. Eng.*, 1982,21(3):427-431.
- [4] LIU D B. Measuring the positions of linear array CCD's elements by means of digital image correla-

- tion [J]. *Opt. Precision Eng.*, 1993, 1(5): 154-160.
- [5] ZHOU P, GOODSON K E. Subpixel displacement and deformation gradient measurement using digital image/speckle correlation [J]. *Opt. Eng.*, 2001, 40(8):1613-1620.
- [6] LI X Z, DAI Q, WANG X J. Digital speckle correlation method of multi-scale wavelet noise reduction [J]. *Opt. Precision Eng.*, 2007, 15(1):57-62. (in Chinese)
- [7] ZHANG J, JIN G C. Application of an improved subpixel registration algorithm on digital speckle correlation measurement [J]. *Optics & Laser Technology*, 2003, 35:533-542.
- [8] CHEN H, YE D, CHEN G, *et al.*. Digital image correlation search method based on genetic algorithm [J]. *Opt. Precision Eng.*, 2007, 15(10): 1633-1637.
- [9] PAN B, XIE H M, XU B Q, *et al.*. Development of sub-pixel displacements registration algorithms in digital image correlation [J]. *Advances in Mechanics*, 2005, 35(3):345-352. (in Chinese)
- [10] MA S P, JIN G C. New correlation coefficient designed for digital image correlation method (DSCM)[J]. *SPIE*, 2003, 5058:25-33.
- [11] PAN B, XU B Q, CHEN D, *et al.*. Sub-pixel registration using quadratic surface fitting in digital image correlation [J]. *Acta Metrologica Sinica*, 2005, 26(2):128-134.
- [12] LI ZH. *Study on Figure Measurement System for Large Aspheres in Synchrotron Radiation* [D]. Beijing: Department of Precision Instruments and Mechanology Tsinghua University.
- [13] CAI K B, WANG CH L, CHEN Z H. A method for generating standard Gaussian white noise sequences [J]. *Proceedings of the CSEE*, 2006, 24(12):207-211.
- [14] XU J C, XU Q, CAI L Q, *et al.*. A new fringe-pattern preprocess method based on median spin filtering [J]. *High Power Laser and Particle Beams*, 2006, 18(1):69-72.

Brief introduction of author:



LANG Zhi-guo(1978—), male, Ph. D. candidate, professional research fields are optical detection of large aperture aspheric surface, image processing, *etc.*. E-mail: lzg666ok@163.com

Brief introduction of supervisor:



TAN Jiu-bin(1955—), male, professor, Ph. D. tutor, professional research fields are ultra-precise measurement technology and instrumentation engineering, technique of optical-mechanical-electrical integration, *etc.*. E-mail: jbtan@hit.edu.cn